www.MaterialsViews.com

Out-of-Plane Plasmonic Antennas for Raman Analysis in Living Cells

*Rosanna La Rocca, Gabriele C. Messina, Michele Dipalo, Victoria Shalabaeva, and Francesco De Angelis**

Currently, many techniques were developed for the investigations of cell cultures[1a–c] because it represents a fundamental tool for the detection of anomalies and early diagnosis of diseases, or more in general to investigate cell response to external stimuli.[2] Analyses of proteins, deoxyribonucleic acid (DNA) and ribonucleic acid (RNA) are possible using quantitative mass spectrometry,[3] western blotting,[4] polymerase chain reaction (PCR),[5] and other conventional molecular biology approaches that need the degradation or the fixing of cells. Presently, the most frequently used method to study molecular dynamics into living cells is fluorescence analysis, being a cost-effective technique that allows fast responses and high sensitivity. However, this approach still presents some intrinsic problems related to its working principles. For instance, fluorescence-based analyses need specific biochemical protocols aiming at labeling molecules or tissues of interest. This fact imposes limitations on the number of molecules investigated and it also requires specific skills in biochemistry. Furthermore, the exploitation of labels can present issues related to cytotoxicity, especially when enhancers such as quantum dots are used.[2]

Among recently proposed alternative techniques, Raman spectroscopy is one of the most interesting. In fact, it is a label free technique in which biomolecules can be distinguished according to their spectroscopic fingerprint, without the need of any additional marker, thus overcoming issues related to toxicity and biochemical skills. Raman spectroscopy can give detailed information about the whole chemical environment and it offers the possibility of mapping the distribution of cellular components in space and time.[6a–d] On the other hand, Raman scattering phenomena present cross-sections in the order of 10^{-30} cm^2, relatively low if compared with absorption cross-sections of fluorescence ($\approx 10^{-16}$ cm^2).[7] Such a low sensitivity can be partially overcome by using surface plasmon polaritons, usually called plasmons, as electrical field enhancers in a process known as surface enhanced Raman scattering (SERS).[8] Literature reports several examples of SERS analysis of living cells obtained through the use of noble metal nanoparticles (NPs) as electric field enhancers.[9a–e] For example, the use of gold NPs helped the observation of molecular changes during cell apoptosis,[10] and transport phenomena[9e] and were also used for molecular imaging of living cells,[11a,b] cellular phenotyping,[12] and for in vivo SERS measurements.[13] However, also this approach presents some major limitations. First, NPs can present high cytotoxicity and can cause biological contaminations. Different sterilization techniques were evaluated but most of them can cause massive aggregation of the nanoparticles followed by precipitation.[14] In this view, the general approach to use surfactants to prevent NPs aggregation is not useful, since surface functionalization, even if carefully controlled,[15] reduces the amount of available SERS sites and it introduces a background in the Raman signal that makes the lowering of the signal to noise ratio. On the other side, even if NPs present random and unsteady distribution inside or around the living cells, they can provide information related to specific targeted areas of the cell. Unlike NPs, nanostructured surfaces do not need surface functionalization, and they can be designed for providing intense plasmonic hot spots in well-defined spatial distributions.[16] Cells can be easily cultured on those surfaces which offer high biocompatibility and do not require advanced skills to be managed.

These intriguing properties have increased the interest for elongated plasmonic nanostructures and recent literature shows several examples of ultrasensitive mapping,[17] biodetection,[18a,b] cellular investigation,[19a,b] and manipulation.[20a,b] Unfortunately, cells tend to adhere on the metal surface in random points thus frustrating the capability of exploiting a set of well-defined plasmonic hot spots as predictable and stable detection points. Moreover, due to the adhesion of the cellular membrane, spectroscopic information is only limited to extracellular species.

Here we show that 3D SERS substrates presenting vertical plasmonic nanoantennas protruding from the substrate plane can overcome the main limitations introduced above thus enabling the chemical analysis of living cells by means of Raman spectroscopy. In the following we demonstrate that cells cultured on such a 3D surface spontaneously grab the vertical nanostructures in predictable points that coincide with

Dr. R. La Rocca, Dr. G. C. Messina, Dr. M. Dipalo, V. Shalabaeva, Dr. F. De Angelis
Istituto Italiano di Tecnologia
via Morego 30, 16163 Genoa, Italy
E-mail: francesco.deangelis@iit.it

DOI: 10.1002/smll.201500891

small NANO MICRO

the plasmonic hot spots, without the need of chemical functionalization. The performance of the 3D antennas was tested with mouse fibroblasts NIH/3T3 as in vitro model, while their biocompatibility and morphology was tested both on NIH/3T3 cells and mouse neuroblastoma cells (Neuro2a or N2a).

Vertical 3D nanoantennas were obtained through a recently developed fabrication method based on focused ion beam technology whose details can be found in previous works.[21a–c] For sake of clarity we reported in **Figure 1**a a scanning electron microscopy (SEM) image of a representative vertical antenna, whereas additional details are described in the Supplementary Information. In this work a silver/gold bilayer was used as coating for the nanoantennas, since the underlying silver offers the already proven high plasmonic enhancement, while the external thin gold coating leads to high biocompatibility and chemical stability.[22]

The difference between vertical and planar approach is sketched in Figure 1b. In case of vertical nanostructures, cells tightly adhere to the tips of the plasmonic antennas, thus putting in close contact the cell membrane with the plasmonic hot spots. The distance between the plasma membrane and the surface of the antenna is on the nanometer scale, leading to a full exploitation of the plasmonic enhancement of Raman signal. In this way the contact point is well predictable and it coincides with the plasmonic hot spot. Indeed, planar SERS substrates can provide such a tight adhesion, but contact points are randomly distributed, not easily predictable, and not necessarily correspondent to the spatial distribution of plasmonic hot spots. We also notice that, although 3D nanoantennas are more expensive than planar ones, or other plasmonic or biosensing devices,[23a–c] they were demonstrated to be recyclable.[22] Furthermore they can provide good sterility: in fact, potential biological contaminants can be easily removed from nanoantennas by UV exposure.

Following this approach, different substrates were prepared by fabricating 1.7 μm high antennas with different spatial arrangement (squared, triangular, and random) and different pitch (2–5 μm). N2a and NIH/3T3 cell lines were cultured on those 3D substrates without adhesion factors (such as poly-lysine) for 2 days in vitro (2 DIVs) with the aim of evaluating adhesion and proliferation mechanism. Statistical analysis of cell adhesion on the various nanoantennas pitch and spatial distribution were performed. In Figure 1 optical images of cells cultured on different antennas arrays are reported (panels (b)–(e): squared arrays with variable pitches; panels (f)–(h): comparison of squared, triangular, and random arrangements).

As a first observation, it is clear that both cell lines grow and proliferate well on the substrates with nanoantennas acting as mechanical support. In fact, we have positively observed that cells tend to settle preferentially on the antennas arrays rather than on the unpatterned surface. No clear dependences on the

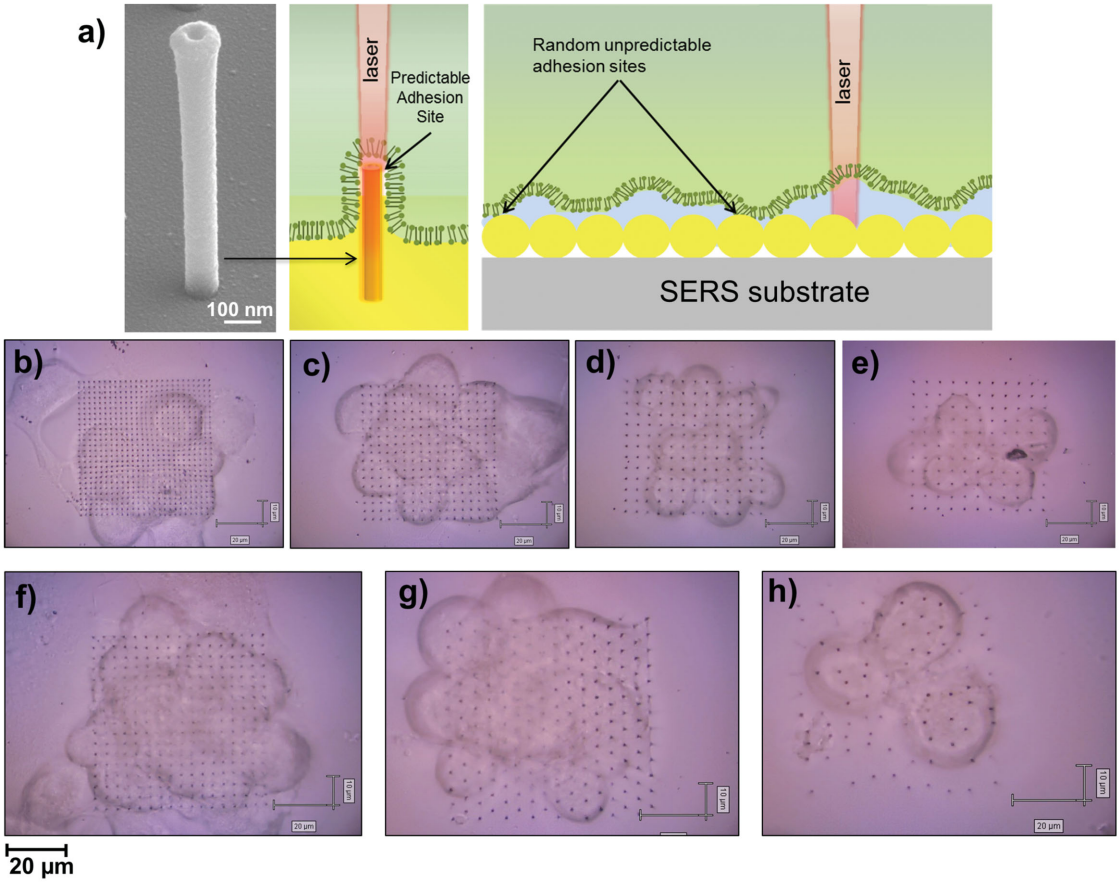

Figure 1. Neuro-2a cells growth on nanoantenna arrays at different pitches: a) Sketches representation of the cell/nanoantenna (left) and cell/planar SERS substrate (right) systems; b) 2 μm, c,g) 3 μm, d,f) 4 μm, e,h) 5 μm, f–h) patterns with squared, triangle, and random distribution, respectively. Scale bar: 20 μm.

www.MaterialsViews.com

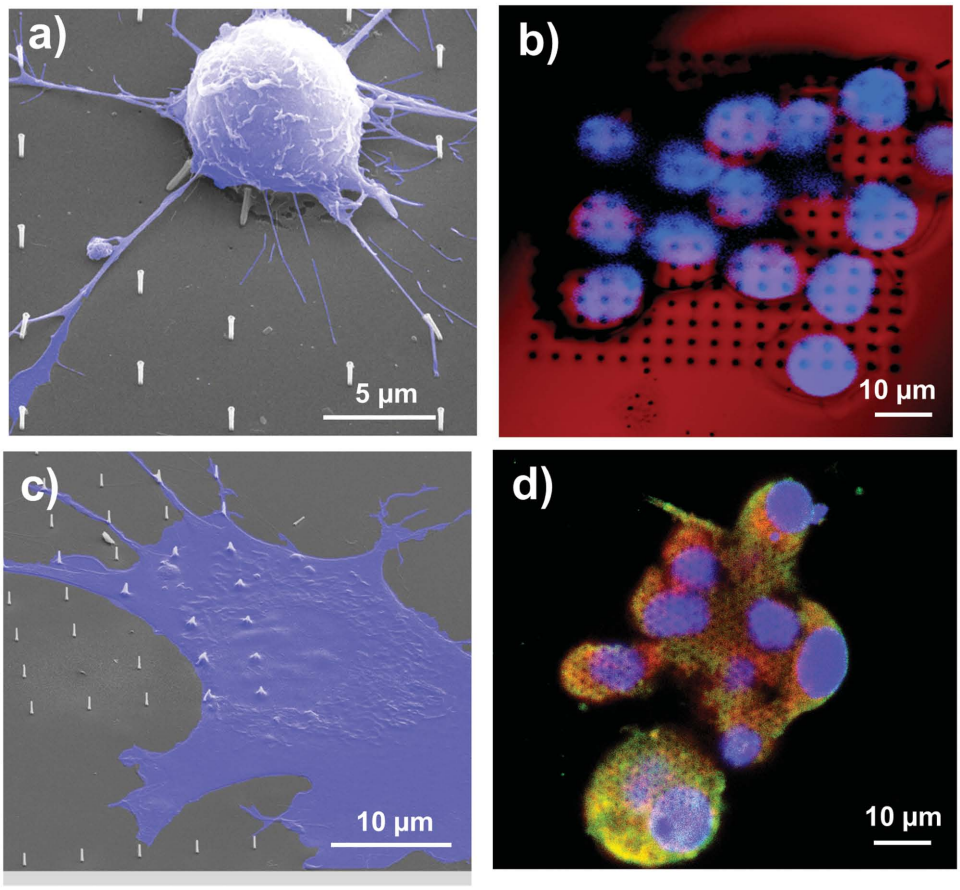

Figure 2. SEM and fluorescence images of a,b) Neuro-2a and c,d) NIH/3T3 cells cultured on 3D nanoantennas. The panels (a) and (c) show interactions between filopodia and antennas arrays and in particular the NIH/3T3 (c) appears lying down on surface nanostructured; (b) neuro-2a nuclei stained with Dapi dye (blue) on antennas; (d) NIH/3T3 stained for the F-actin (red), the vinculin protein (green) and nuclei (blue). Scale Bars: 5 µm (a), 10 µm (b, c, and d).

antenna spatial arrangements or pitches were evidenced in the range of parameters we investigated. We notice that since adhesion efficiency does not depend on the pattern geometry, it would be possible to use the antennas spatial arrangement for achieving diffractive coupling effects (or grating effects) that maximize the plasmonics enhancement.[24]

In order to qualitatively estimate the efficiency of cell adhesion on the nanoantennas, we performed confocal imaging of cells placed on nanoantennas disposed with squared arrangement, as reported in **Figure 2**b,d. The fluorescence images show the vinculin protein expression and F-actin filaments distribution inside N2a and NIH/3T3 cell lines. As reported in literature, the focal adhesion formation, as well as cell mobility, is controlled by vinculin,[25] which is involved in the regulation of cell survival and growth[26a,b] and it has the ability to bind F-actin filaments. Like vinculin, also F-actin plays an important role in cell morphology, cell motility, and muscle function.[27] Based on these results we can confidently state that N2a and NIH/3T3 cells interact strongly with nanoantennas and grow easily on them. A further insight of the in vitro development morphology distribution has been obtained with SEM and such results are reported in Figure 2b,d.

After 2 DIVs on the nanoantennas, the cells show good adhesion and optimal morphology, forming strong connections with nanoantennas (Figure 2a,c). Moreover, the cell bodies appear well supported by nanoantennas and the ramifications well anchored to surrounding nanoantennas (Figure 2a,c). In Figure 2a,c we observe that few nanoantennas are broken or bent; this effect is entirely due to the mechanical stress of dehydration required for SEM imaging: in fact, all nanoantennas are standing vertically before dehydration. Viability assays were performed to test the biocompatibility, after 2 DIVs the percentage of viable cells was approximately 100% (Figure S1, Supporting Information).

Finally, after the evaluation of adhesion and biocompatibility we assessed the capabilities of the 3D nanostructures in terms of Raman analyses. Raman measurements were performed on both NIH/3T3 and N2a living cells still immersed in their cell media. Spectra were taken at different points of the cells resting on the nanoantennas and show different vibrational features related to various membrane cell components.

We did not notice significant differences or anomalies between results coming from the two different lines, so for sake of brevity and clarity here we are going to discuss in details only data related to mouse fibroblasts NIH/3T3.

Figure 3a compares SERS spectra obtained on cells laying on the antenna (red line in figure) and on flat substrate (black line). SERS measurements were carried out using a 60× water immersion objective, an excitation laser at λ = 785 nm, with 10 mW of nominal laser power, and 10 s

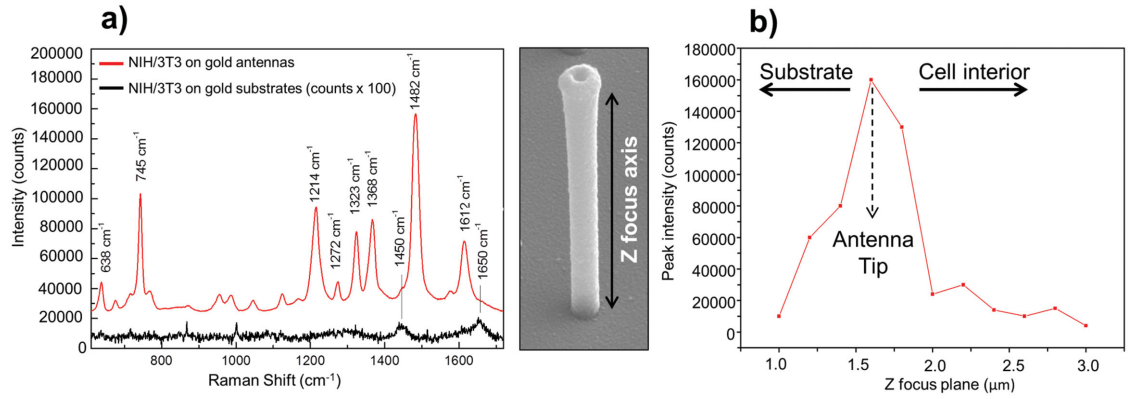

Figure 3. a) (left) SERS spectra obtained on NIH/3T3 cell lying respectively on the top of the antenna (red line) and on the bottom of the substrate (black line). Measurements were performed with a Renishaw InVia micro-Raman microscope and all data were analyzed with Origin 9.1 (OriginLab, USA) software program; (a) (right) SEM image of a 3D nanoantennas. b) Raman counts of the peak at 1482 cm^{-1} in respect to the focus plane along the antenna height.

of acquisition time. The strong signal intensities associated to cells on antennas with respect to those coming from the substrate is a clear evidence of the high efficiency of the antennas as enhancers of the electromagnetic field in the NIR (near infrared) range.

By comparing peak intensities and measurement parameters, we estimated that cells on nanoantennas present peak intensities 6.5×10^4 higher than that on the silver/gold substrate.

In terms of pure field enhancement, this means that antennas provide a magnification of the incoming electric field 15 times greater than that provided by the rough silver/gold substrate, corresponding to an absolute enhancement factor of about 45 times the amplitude of the incoming laser field.

Even if the latter outcome is in accordance with our previous results concerning the quantification of the enhancement provided by these kinds of antennas.[21a–c] We would like to underline that a precise estimation of the total signal enhancement should also include other parameters.

For example, most enhanced peaks, as the one at 1482 cm^{-1}, do not present a counterpart on the substrate spectrum, thus preventing the calculation of a maximum enhancement value.

The presence of different features in the Raman spectra from the same cellular system can be attributed to different interactions of molecules with the surface, resulting in different relative intensity of the peaks. Indeed, the reconfiguration of the lipidic membrane results in a change of the spectrum both in space[10b] and time,[28] making hard to compare spectra acquired in two different positions at different moments.

In general, we noticed that spectra collected on vertical nanoantennas are always stronger than those collected on the planar substrate. By assuming the presence of SERS enhancement for molecules on a region of ≈15 nm from the surface,[29] we consider appropriate to attribute a lack of enhancement from the substrate to a softer contact of the cell on it.

The large number of vibrational features reported in Figure 3a can supply a large amount of information for the study of the cell behavior. According to the current literature we reported possible attributions of peaks in **Table 1**. The most intense peaks arise from the ring modes of tryptophan (745 cm^{-1}) and other aromatic aminoacids (at 1214 cm^{-1}).[30] Other intense signal can be associated to Amide III alpha helix (1323 cm^{-1}), amide II (1482 cm^{-1}), and double bonds from tyrosine and tryptophan (1612 cm^{-1}) while, the two peaks at 1214 and 1272 cm^{-1} are characteristic of protein secondary structures (α-helix and β-sheet).[31a,b] The fact that these signals are associated to groups including nitrogen atoms is a clear evidence of the plasmonic origin of the signal

Table 1. Positions of the peaks reported in Figure 3 and their possible attribution obtained by comparison with literature data.

Peak position [cm^{-1}]	Possible attribution
638	C–C twist phenylalanine, tyrosine
677	
726	C–S protein, twist CH_2, rocking A (Adenine)
745	Ring tryptophan
768	Ring tryptophan
871	C–C–N sym. stretching of lipids, C–O–C carbohydrates
954	Hydroxyapatite, carotenoid, cholesterol
988	C–C BK stretching
1044	Phenylalanine
1123	O–P–O DNA backbone
1154	Tyrosine
1214	C–C_6H_5, tyrosine, tryptophan, phenylalanine
1272	Saccharides, proteins
1323	Amide III alpha helix
1368	CH_3 symmetric stretching of lipids
1450	CH_2, CH_3 deformation, phospholipids
1482	Amide II
1572	G, A (Guanine, Adenine)
1612	C=C tyrosine, tryptophan
1650	Amide I

enhancement, due to the strong interaction of nitrogen with gold.[32]

In some cases, while the Raman spectrum collected out of the antenna (Figure 3, black curve) shows strong Raman bands at 1450 cm^{-1} (protein CH deformation vibration, phospholipids)[33a,b] and 1650 cm^{-1} (amide I), such features are weakly enhanced (in the case of 1450 cm^{-1}) or not enhanced at all in the SERS spectrum. Same behavior has been already found in literature,[34] confirming a selectivity behavior of SERS approach in the investigation of cellular membranes.

The reported spectra provide also structural information related to proteins. The alpha helix structure (1323 cm^{-1}) is often found in proteins related to anchor proteins or to ion channels, while the feature at 988 cm^{-1} corresponds to BK (Big Potassium) channels. Further structural information also offered the presence of the cholesterol peak (954 cm^{-1}), which is involved in the fluidity of the cellular membrane. It is also interesting to notice the presence of a DNA backbone peak (1123 cm^{-1}). The simultaneous absence of the band at 735 cm^{-1}, corresponding to the adenine ring-breathing mode, means that native and not denatured DNA is present,[34] indicating the good state of the cell. In addition to information outlined above, the proposed approach can give many interesting information of processes occurring on the cell membrane or cellular activities in general. For instance, it could represent a novel route for monitoring the membrane phenotypic changes in primary cells, which could have a loss of phenotype at increasing time in culture.[35] Also, it could enable the study of secondary structures of membrane glycoproteins or the changes of channels, which regulate the flow of charged ions inside the cell. Finally, it might be interesting for monitoring variations of cholesterol within the phospholipid bilayer of living cells.

In order to definitively confirm that the recorded Raman signals come only from the tip (interface between plasmonic hot spot and cell membrane), we acquired a set of spectra by changing the focus of the collection objective along the vertical direction. In Figure 3b the intensity of the peak is reported at 1482 cm^{-1} with respect to the focus plane along the antenna height. As expected, the spectrum acquired on the antenna tip presents ten times more counts than the ones collected along the antenna body. We would like to underline that supplied laser powers did not contribute to damage or breaking of the cellular membrane as reported in other works.[19b] Indeed, such events should have generated a strong decrease of the Raman intensity in consecutive measurements, due to a vanishing of the spectrum related to membrane. Moreover, we never noticed any peaks related to nucleic acids or other cytoplasmic components.

In summary, we showed that vertical 3D plasmonic antennas are very efficient tools for the chemical analysis of living cells. The tight adhesion between cells and antennas enables sensitive SERS analysis of cell membrane elements in well-defined and predictable points. Moreover, the silver/gold bilayer coating allowed to combining high plasmonic field enhancement with biocompatibility. By exploiting these features, we were able to acquire SERS Raman spectra of living cells using near-IR source, with very low laser intensities, and without perturbing the culture with external contaminants. Even in these mild conditions, obtained spectra presented peaks with more than 10^5 counts and with an enhancement approximately 40/45 times the amplitude of incident field. This is a promising result in the view of precise quantitative analysis of all biomolecules present in the cells environment. Finally we stress the fact that cells are cultured with standard procedures without any additional substances, tools, or skills, thus making this technique fully compatible with the majority of protocols currently used for in vitro investigations.

Supporting Information

Supporting Information is available from the Wiley Online Library or from the author.

Acknowledgements

R.L.R., G.C.M., and M.D. contributed equally to this work. The research leading to these results received funding from the European Research Council under the European Union's Seventh Framework Programme (FP/2007–2013)/ERC Grant Agreement No. [616213], CoG: Neuro-Plasmonics.

[1] a) J. L. Zabzdyr, S. J. Lillard, *Anal. Chem.* **2001**, *73*, 5771; b) A. B. Anderson, J. Gergen, E. A. Arriaga, *J. Chromatogr. B. Analyt. Technol. Biomed. Life Sci.* **2002**, *769*, 97; c) S. Zhao, Y. Huang, M. Shi, R. Liu, Y.-M. Liu, *Anal. Chem.* **2010**, *82*, 2036.
[2] I. H. Stevenson, K. P. Kording, *Nat. Neurosci.* **2011**, *14*, 139.
[3] S. E. Ong, M. Mann, *Nat. Chem. Biol.* **2005**, *1*, 252.
[4] H. Towbin, T. Staehelin, J. Gordon, *Proc. Natl. Acad. Sci. USA* **1979**, *76*, 4350.
[5] C. A. Heid, J. Stevens, K. J. Livak, P. M. Williams, *Genome Res.* **1996**, *6*, 986.
[6] a) M. Li, J. Xu, M. Romero-Gonzalez, S. A. Banwart, W. E. Huang, *Curr. Opin. Biotechnol.* **2012**, *23*, 56; b) G. J. Puppels, F. F. de Mul, C. Otto, J. Greve, M. Robert-Nicoud, D. J. Arndt-Jovin, T. M. Jovin, *Nature* **1990**, *347*, 301; c) H. J. van Manen, Y. M. Kraan, D. Roos, C. Otto, *Proc. Natl. Acad. Sci. USA* **2005**, *102*, 10159; d) C. Matthäus, T. Chernenko, J. A. Newmark, C. M. Warner, M. Diem, *Biophys. J.* **2007**, *93*, 668.
[7] S. R. Emory, R. A. Jensen, T. Wenda, M. Han, S. Nie, *Faraday Discuss.* **2006**, *132*, 249.
[8] A. Campion, P. Kambhampati, *Chem. Soc. Rev.* **1998**, *27*, 241.
[9] a) K. C. Huang, K. Bando, J. Ando, N. I. Smith, K. Fujita, S. Kawata, *Methods* **2014**, *68*, 348; b) N. I. Smith, K. Mochizuki, H. Niioka, S. Ichikawa, N. Pavillon, A. J. Hobro, J. Ando, K. Fujita, Y. Kumagai, *Nat. Commun.* **2014**, *5*, 5144; c) K. Fujita, S. Ishitobi, K. Hamada, N. I. Smith, A. Taguchi, Y. Inouye, S. Kawata, *J. Biomed. Opt.* **2009**, *14*, 024038; d) K. Kneipp, A. S. Haka, H. Kneipp, K. Badizadegan, N. Yoshizawa, C. Boone, K. E. Shafer-Peltier, J. T. Motz, R. R. Dasari, M. S. Feld, *Appl. Spectroscop.* **2002**, *56*, 150; e) J. Ando, K. Fujita, N. I. Smith, S. Kawata, *Nano Lett.* **2011**, *11*, 5344.
[10] a) B. Kang, L. A. Austin, M. A. El-Sayed, *ACS Nano* **2014**, *8*, 4883.
[11] a) A. F. Palonpon, J. Ando, H. Yamakoshi, K. Dodo, M. Sodeoka, S. Kawata, K. Fujita, *Nat. Protoc.* **2013**, *8*, 677; b) J. W. Kang, P. T. C. So, R. R. Dasari, D.-K. Lim, *Nano Lett.* **2015**, *15*, 1766.

[12] A. Huefner, W.-L. Kuan, R. A. Barker, S. Mahajan, *Nano Lett.* **2013**, *13*, 2463.
[13] C. L. Zavaleta, B. R. Smith, I. Walton, W. Doering, G. Davis, B. Shojaei, M. J. Natan, S. S. Gambhir, *Proc. Natl. Acad. Sci. USA* **2009**, *106*, 13511.
[14] E. Memisoglu-Bilensoy, A. A. Hincal, *Int. J. Pharm.* **2006**, *311*, 203.
[15] R. Randazzo, A. Di Mauro, A. D'Urso, G. C. Messina, G. Compagnini, V. Villari, N. Micali, R. Purrello, M. E. Fragalà, *J. Phys. Chem. B* **2015**, *119*, 4898.
[16] M. Chirumamilla, A. Toma, A. Gopalakrishnan, G. Das, R. P. Zaccaria, R. Krahne, E. Rondanina, M. Leoncini, C. Liberale, F. De Angelis, E. Di Fabrizio, *Adv. Mater.* **2014**, *26*, 2353.
[17] F. De Angelis, G. Das, P. Candeloro, M. Patrini, M. Galli, A. Bek, M. Lazzarino, I. Maksymov, C. Liberale, L. C. Andreani, E. Di Fabrizio, *Nat. Nanotechnol.* **2010**, *5*, 67.
[18] a) F. De Angelis, F. Gentile, F. Mecarini, G. Das, M. Moretti, P. Candeloro, M. L. Coluccio, G. Cojoc, A. Accardo, C. Liberale, R. P. Zaccaria, G. Perozziello, L. Tirinato, A. Toma, G. Cuda, R. Cingolani, E. Di Fabrizio, F. De Angelis, E. Di Fabrizio, *Nat. Photon.* **2011**, *5*, 682; b) J.-A. Huang, Y.-Q. Zhao, X.-J. Zhang, L.-F. He, T.-L. Wong, Y.-S. Chui, W.-J. Zhang, S.-T. Lee, *Nano Lett.* **2013**, *13*, 5039.
[19] a) R. Yan, J.-H. Park, Y. Choi, C.-J. Heo, S.-M. Yang, L. P. Lee, P. Yang, *Nat. Nanotechnol.* **2012**, *7*, 191; b) G. Lu, H. De Keersmaecker, L. Su, B. Kenens, S. Rocha, E. Fron, C. Chen, P. Van Dorpe, H. Mizuno, J. Hofkens, J. A. Hutchison, H. Uji-i, *Adv. Mater.* **2014**, *26*, 5124.
[20] a) A. K. Shalek, J. T. Robinson, E. S. Karp, J. S. Lee, D.-R. Ahn, M.-H. Yoon, A. Sutton, M. Jorgolli, R. S. Gertner, T. S. Gujral, G. MacBeath, E. G. Yang, H. Park, *Proc. Natl. Acad. Sci. USA* **2010**, *107*, 1870; b) C. Xie, Z. Lin, L. Hanson, Y. Cui, B. Cui, *Nat. Nanotechnol.* **2012**, *7*, 185.
[21] a) F. De Angelis, M. Malerba, M. Patrini, E. Miele, G. Das, A. Toma, R. P. Zaccaria, E. Di Fabrizio, *Nano Lett.* **2013**, *13*, 3553; b) G. C. Messina, M. Malerba, P. Zilio, E. Miele, M. Dipalo, L. Ferrara, F. De Angelis, *Beilstein J. Nanotechnol.* **2015**, *6*, 492; c) M. Dipalo, G. C. Messina, H. Amin, R. La Rocca, V. Shalabaeva, A. Simi, A. Maccione, P. Zilio, L. Berdondini, F. De Angelis, *Nanoscale* **2015**, *7*, 3703.
[22] A. Gopalakrishnan, M. Chirumamilla, F. De Angelis, A. Toma, R. P. Zaccaria, R. Krahne, *ACS Nano* **2014**, *8*, 7986.
[23] a) E. Miele, M. Malerba, M. Dipalo, E. Rondanina, A. Toma, F. De Angelis, *Adv. Mater.* **2014**, *26*, 4179; b) R. Intartaglia, S. Beke, M. Moretti, F. De Angelis, A. Diaspro, *Lab Chip* **2015**, *15*, 1343; c) G. C. Messina, P. Wagener, R. Streubel, A. De Giacomo, A. Santagata, G. Compagnini, S. Barcikowski, *Phys. Chem. Chem. Phys.* **2013**, *15*, 3093.
[24] B. Auguié, W. L. Barnes, *Phys. Rev. Lett.* **2008**, *101*, 143902.
[25] B. Lifschitz-Mercer, B. Czernobilsky, E. Feldberg, B. Geiger, *Hum. Pathol.* **1997**, *28*, 1230.
[26] a) J. L. R. Fernández, B. Geiger, D. Salomon, A. Ben-Ze'ev, *Cell Motil. Cytoskeleton* **1992**, *22*, 127; b) J. L. R. Fernández, B. Geiger, D. Salomon, A. Ben-Ze'ev, *J. Cell Biol.* **1993**, *122*, 1285.
[27] J. Stricker, T. Falzone, M. L. Gardel, *J. Biomech.* **2010**, *43*, 9.
[28] R. W. Taylor, F. Benz, D. O. Sigle, R. W. Bowman, P. Bao, J. S. Roth, G. R. Heath, S. D. Evans, J. J. Baumberg, *Sci. Rep.* **2014**, *4*, 5940.
[29] M. D. Hodges, J. G. Kelly, A. J. Bentley, S. Fogarty, I. I. Patel, F. L. Martin, N. J. Fullwood, *ACS Nano* **2011**, *5*, 9535.
[30] A. I. M. Athamneh, R. S. Senger, *Appl. Environ. Microbiol.* **2012**, *78*, 7805.
[31] M. A. Ochsenkühn, P. R. T. Jess, H. Stoquert, K. Dholakia, C. J. Campbell, *ACS Nano* **2009**, *3*, 3613; b) E. Podstawka, Y. Ozaki, L. M. Proniewicz, *Appl. Spectrosc.* **2004**, *58*, 1147.
[32] Y. Ortega, N. C. Hernandez, E. Menéndez-Proupin, J. Graciani, J. F. Sanz, *Phys. Chem. Chem. Phys.* **2011**, *13*, 11340.
[33] M. D. Hodges, J. G. Kelly, A. J. Bentley, S. Fogarty, I. I. Patel, F. L. Martin, N. J. Fullwood, *ACS Nano* **2011**, *5*, 9535; b) D. Manno, E. Filippo, R. Fiore, A. Serra, E. Urso, A. Rizzello, M. Maffia, *Nanotechnology* **2010**, *21*, 165502.
[34] K. Kneipp, A. S. Haka, H. Kneipp, K. Badizadegan, N. Yoshizawa, C. Boone, K. E. Shafer-Peltier, J. T. Motz, R. R. Dasari, M. S. Feld, *Appl. Spectrosc.* **2002**, *56*, 150.
[35] R. J. Swain, S. J. Kemp, P. Goldstraw, T. D. Tetley, M. M. Stevens, *Biophys. J.* **2010**, *98*, 1703.

Received: April 1, 2015
Revised: May 18, 2015
Published online: June 26, 2015

